Single-molecule magnet behavior in luminescent carbazolyl Dy(III) octahedral complexes with a quasi linear N^{-}-Dy-N^{-} angle.

Jérôme Long*,[a] Alexander N. Selikhov,[b,c] Ekaterina Mamontova,[a] Konstantin A. Lyssenko,[c,d] Yannick Guari,[a] Joulia Larionova[a] and Alexander A. Trifonov*[b,c]

We report the synthesis, photoluminescent and magnetic investigations of two octhadral dysprosium complexes $[DyR_2(py)_4][BPh_4]\cdot 2py$ (1) and $[DyR_2(THF)_4][BPh_4]$ (R = carbazolyl, py = pyridine, THF = tetrahydrofuran) exhibiting a quasi linear N-Dy-N angle in the axial direction, suitable to provide a coordination environment allowing a zero-field slow relaxation of the magnetization.

Coordination complexes based on lanthanide(III) ions have recently emerged as an exciting field in molecular materials due to their tremendous physical properties related to the combination of a strong spin-orbit coupling with a crystal-field effect, which results in a large anisotropy for some lanthanide ions. For instance, such lanthanides complexes could exhibit a magnetic bistability, usually called Single-Molecule Magnets (SMMs) behaviour, making them as potential candidates for applications in data storage, spintronics or quantum computing.[1-4] Yet, such feature could not be observed in all lanthanide complexes since the origin of the phenomenon requires the presence of a large anisotropic barrier that opposes two magnetic states ($\pm m_J$), which can be controlled by the coordination environment of the lanthanide ion. It is commonly accepted that in performing SMMs, the energy barrier should be as large as possible and the retention of the magnetization should be achieved in zero field under a so-called blocking temperature.

Among several synthetic strategies aiming to increase the anisotropic barriers, stabilizing the oblate electronic density of some lanthanide ions, such as the Dy^{3+}, by coordination of two negatively charged ligands with short bond lengths along an axial direction and the absence of any ligands in the equatorial plane has been recognized as a powerful approach.[5-6] This strategy permits to maximize the crystal-field splitting when a suitable symmetry is obtained. Hence, major achievements have been reached in the last few years by using coordination and organometallic chemistry concepts,[7-12] pushing back the limits of the magnetic anisotropy in the dysprosium metallocene family[13-14] with magnetic hysteresis observed up to 80 K.[15] On the other hand, the relaxation may be highly impacted by the presence of the Quantum Tunnelling of the Magnetization (QTM), as well as Raman and direct relaxations, which reduce the SMMs performances. Nowadays, upgrading SMMs require determining the parameters affecting the spin-phonon coupling that stand in need to be grasped.[2, 6, 16-19]

Among the different ligands used in coordination chemistry, those involving oxygen or nitrogen donor atoms appear interesting since they may not only stabilize the oblate electronic density of Dy^{3+}, but may also act as antennas to design luminescent SMMs.[20-21] Surprisingly, we realized that the number of high anisotropic barrier SMMs based on amido/imido ligands is still relatively scarce with respect to their alkoxy counterpart,[2] although recent theoretical calculations have predicted an effective energy barrier larger than 4000 K in a two-coordinate imido complex.[22] In this sense, carbazole-based ligands are highly appealing since: i) they provide rigidity owing to the presence of multiple aromatic rings; ii) benefit from great tunability to introduce novel functionalities; iii) they could act as a simple monoanionic amido ligand but also could form π-complexes;[23] iv) the negatively charged character makes them very promising to design SMMs with axial crystal-field. Moreover, carbazole, featuring a rigid plane biphenyl core with wide band gap and high luminescent efficiency presents great opportunities for the synthesis of new emitters.[24-26] Although, derivatives of carbazolyl ligands (mostly tridentate) have been investigated towards lanthanide(III) ions,[27] simple carbazole has mainly been used with divalent lanthanide ions.[28-30] With this in mind, we report herein the synthesis, structure, photoluminescent and magnetic studies of two octahedral Dy(III) carbazolyl-based complexes with a quasi linear (carbazolyl)N^{-}-Dy-N^{-}(carbazolyl) arrangement, exhibiting a Dy^{3+} luminescence associated with a SMM behaviour.

Our synthetic strategy relies on the formation of a cationic dicarbazolyl complex $[DyR_2]^{+}$ moiety (R^{-} = carbazolyl) in association with a bulky non-coordinating anion. Thus, complexes $[DyR_2(py)_4][B(C_6H_5)_4]\cdot 2py$ (**1**) (py = pyridine) and $[DyR_2(THF)_4][B(C_6H_5)_4]$ (**2**) (THF = tetrahydrofuran) were synthesized by an alkane elimination protocol reacting Dy(*o*-$Me_2NC_6H_4CH_2)_3$ with two equivalents of carbazole and one equivalent of $[NHEt_3][BPh_4]$ (Scheme S1). Subsequent recrystallization from a py/hexane mixture or hot THF allowed obtaining single crystalline samples of **1** and **2**, respectively.

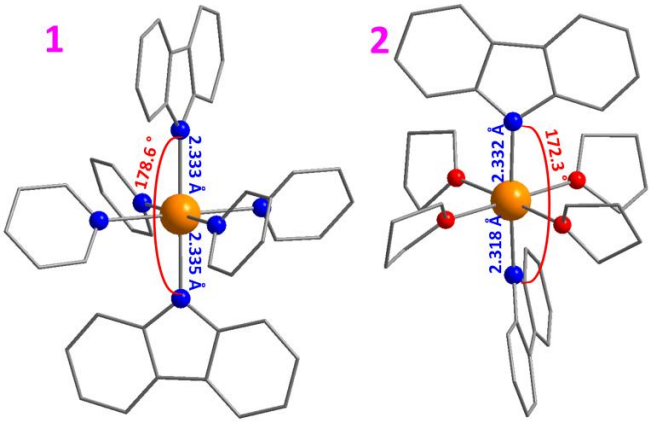

Fig. 1. Left: Molecular structure of the complex $[DyR_2(py)_4]^+$ in **1**. Right: Molecular structure of the complex $[DyR_2(THF)_4]^+$ in **2**. Colour code: orange, Dy; red, O; grey, C. Hydrogen atoms and the $[BPh_4]^-$ moieties have been omitted for clarity.

X-Ray diffraction analyses indicate that **1** and **2** crystallize in the orthorhombic *Pnma* and trigonal $R\overline{3}$ space groups, respectively, with a unique crystallographic complex within the asymmetric unit (Table S1). In **1**, both cation and anion occupy the special position on the mirror plane that coincides with one carbazolyl ligand and crosses the second one. Both complexes exhibit an octahedral geometry (see Shape Analysis, Table S2) with two R^- located in the *trans* axial position and four solvates molecules (py and THF for **1** and **2**, respectively) in the basal plane (Fig. 1). The shortest distances involve two carbazolyl ligands in axial position with Dy-N(R) distances of 2.333(3)/2.335(3) and 2.318(4)/2.332(4) Å for **1** and **2**, respectively. As expected, the Dy-O distances in **2** are relatively close (ranging from 2.318(3) to 2.344(3) Å) to those involving the carbazolyl ligands, while the Dy-N(py) distances in **1** are much longer (2.470(2) and 2.486(2) Å). Hence, a compressed octahedral geometry could be observed for **1** whereas **2** exhibits a much more regular one. Remarkably, the N-Dy-N angle of 178.6(1)° in **1** is closer to the linearity than the one found in **2** (172.3(1)°). The crystal packing analysis indicates that the two uncoordinated solvate pyridine in **1** strongly interact with the carbazolyl ligands through π-π interactions with the shortest C···C contacts equal to 3.38 Å. The shortest Dy-Dy intermolecular distances in the crystals are equal to 9.947 and 10.619 Å for **1** and **2**, respectively (Fig. S1).

The magnetic properties of **1** and **2** were investigated in both, static and dynamic modes by using a SQUID MPMS-XL magnetometer. The room temperature χT values of 14.14 and 14.51 $cm^3.K.mol^{-1}$ for **1** and **2**, respectively, are in accordance with the theoretical value of 14.17 $cm^3.K.mol^{-1}$ ($^6H_{15/2}$) expected for a unique Dy^{3+} ion. Upon cooling, both χT *vs*. *T* curves show a monotonous decrease which reflects the thermal depopulation of the m_J levels (Fig. S2). Then, below 12 K, a dramatic decrease could be observed. The field dependence of the magnetization at 1.8 K and under 70 kOe shows a value of 5.90 and 5.66 *N*β for **1** and **2**, respectively, without any saturation, indicating the presence of a magnetic anisotropy (Insert of Fig. S2). The sigmoidal shape of the *M vs. H* curves at low fields may suggest a flip of the Dy^{3+} spins under an applied magnetic field or the occurrence of dipolar interactions. Additionally, a magnetic bistability could be evidenced in the hysteresis loops at low temperature (Fig. S3).

Hence, the dynamic of the relaxation was investigated by the measurements of the magnetic susceptibility in alternating current (ac) mode. For both complexes, the frequency dependence of the out-of-phase susceptibility component (χ'') under a zero dc-field reveals a series of single temperature dependent peaks, pointing out the occurrence of a slow relaxation of the magnetization (Fig. 2, Fig. S4). The corresponding Cole-Cole plots (Fig. S5) can be fitted with a generalized Debye model giving moderate α parameter values (< 0.2) indicating a narrow distribution of the relaxation times (Table S3-S4). Remarkably, out-of-phase signals could be observed up to 60 and 50 K for **1** and **2**, respectively (Fig. S6). From these data, the investigation of the relaxation dynamics could be achieved by extracting the temperature dependence of the relaxation time, τ. The canonical $\ln\tau$ *vs.* T^{-1} plot (Fig. 3) reveals a deviation from the linearity upon lowering the temperature indicating the presence of additional relaxation processes. The relaxation at low temperature becomes temperature independent indicating a QTM regime. Remarkably, the relaxation time measured at 2 K for **1** is six times greater with respect to that found for **2**, pointing out a noticeable difference in the relaxation dynamics. The overall data range could be modelled using the following equation: $\tau^{-1} = \tau_0^{-1}\exp(-\Delta/kT) + CT^m + \tau^{-1}_{QTM}$ (Eq. 1).[31] The first term accounts for a thermally activated process, while the second and third ones stand for two-phonon Raman and QTM respectively. The *m* value was fixed to 5, which is one of the possible values observed for Kramers ions.[32] The best fit parameters (Table 1) indicate that the magnetization relaxes trough these three processes. Noticeably, while the Δ values are rather close for **1** and **2**, strong differences in the Raman coefficients and QTM rates could be observed.

With the aim to shortcut the contribution from the QTM, the field dependence of the relaxation time τ at 20 K was investigated (Fig. S7) and modelled with the equation $\tau^{-1} = DH^4T + B_1/(1+B_2H^2) + K$ (Eq. 2, Fig. S8, Table S5),[31] for which the first term accounts for the direct process (for Kramers-ion), the second one for the QTM and the *K* constant for the field-independent Raman and thermally activated processes.

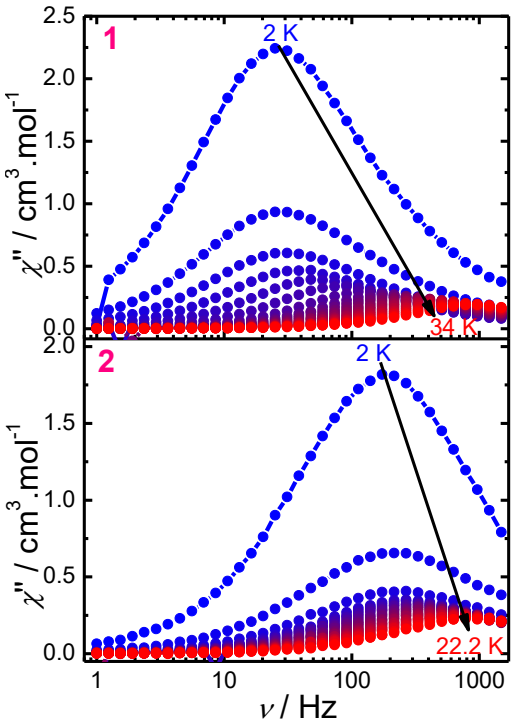

Fig. 2. Frequency dependence of the out-of phase (χ'') susceptibilities for **1** and **2** under a zero dc-field.

The optimum field (field at which the relaxation time is the greatest) was estimated at 1000 Oe and 2000 Oe for **1** and **2**, respectively. Hence, the ac susceptibility data under these dc fields confirmed the reduction of the QTM (Fig. S9-S10, Table S6-S7). The fitting of the temperature dependences of the relaxation time has been performed with the following model: $\tau^{-1} = \tau_0^{-1}\exp(-\Delta/kT) + CT^m + AT$ (Eq. 3) (Fig. 3), in which the third term accounts for the direct process (Table S8). The obtained Δ values are greater with respect to the zero-field data, in particularly for **1**, which may be explained by the presence of a noticeable QTM regime. For both, in-field and zero field data, attempts to fit the temperature dependence of the relaxation time was also performed by fixing the Δ values from the linear fit in the high-temperature region. However poor fitting or unrealistic parameters were obtained (Table S9).

To gain further insights, the orientation of the anisotropic axes for the ground doublet were evaluated using the MAGELLAN[33] software by assuming that a negative charge is localized on the nitrogen atom of the R ligand. As expected, and owing to the negatively charged character of the carbazolyl ligands, these axes are found almost collinear to the (R)N-Dy-N(R)) string (Fig. S11). The deviation angles between the anisotropic axis and (R)N-Dy bonds are equal to 0.05 and 1.14° for **1**, while they are slightly larger for **2** with values of 3.13 and 3.63°. Despite the linear character of the (R)N-Dy-N(R) angle in both compounds, relatively modest anisotropic barriers are found in zero magnetic field, while important differences in the relaxation dynamics are readily observed between two complexes. These features may be rationalized taking into account different parameters. Firstly, whereas **1** exhibits slightly longer Dy-N(R) distances with respect to **2** (2.333(3)/2.335(3) *vs.* 2.318(4)/2.332(4) Å), its exhibits an almost linear (R)N-Dy-N(R) angle of 178.6(1)° against of 172.3(1)°) in **2**, that may explain its higher energy barrier.

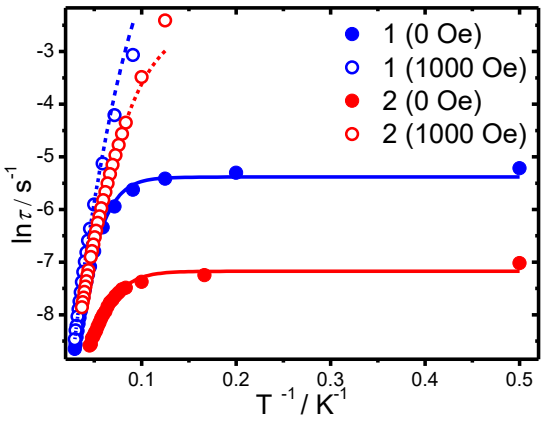

Fig. 3. Temperature dependence of the relaxation time for **1** (blue) and **2** (red) using the ac data at 0 Oe and 1000 Oe. The solid line represents the fit with Eq. 1 (0 Oe) and Eq. 3 (1000 Oe).

Table 1: Fit parameters of the temperature dependence of the relaxation time for **1** and **2**.

Compound	Δ (cm^{-1})	τ_0 (s)	m	C ($s^{-1}.K^{-m}$)	τ_{QTM} (ms)
1 (0 Oe)	50 ± 4	(7 ± 2) × 10^{-5}	5*	(8.3 ± 0.5) × 10^{-6}	4.6 ± 0.4
2 (0 Oe)	40 ± 4	(2.0 ± 0.8) × 10^{-5}	5*	(0.5 ± 1) × 10^{-4}	0.76 ± 0.03

Noticeably, the parameters for **1** may be compared with those of the pentagonal bipyramidal complex $[Dy(OtBu)_2(py)_5][BPh_4]$ presenting a comparable angle of 178.91° (O-Dy-O), but much shorter Dy-O distances (2.110(2)–2.114(2) Å).[11] This difference explains the greater energy barrier of 1250 cm^{-1} in comparison to **1**. More generally, the axial Dy-N(R) distances appear larger in comparison with those found in some phenoxide based SMMs (2.1-2.2 Å)[12, 34] that may decrease the axiality. Secondly, the role of the coordinated solvates in the equatorial plane appears also very important: the Dy-N(py) distances (2.470(2) and 2.486(2) Å) in **1** are much longer than the Dy-O(THF) ones (2.318(3) to 2.344(3) Å) in **2**. Consequently, the presence of these strongly interacting THF moieties in the equatorial plane in **2** provides a greater transverse component. Thus, both the more linear (R)N-Dy-N(R) angle associated with larger bond lengths in the equatorial plane may explain the greater slow relaxation performances of **1** with respect to **2**. More generally, there are rare examples of six-coordinated lanthanide complexes exhibiting a zero-field slow relaxation of their magnetization.[31, 35-40] However, it could be emphasized that **1** and **2** constitute unique examples of octahedral systems with an axial crystal field generated by two negatively charged ligands arranged in *trans*.

Another advantage of the carbazolyl ligands, besides the design of genuine SMMs, consists in their ability to efficiently sensitize the Dy^{3+} ion. Indeed, a dysprosium-based luminescence could be observed at low temperature (77 K) for both complexes (Fig. 4), making these complexes as

multifunctional magneto-luminescent SMMs. The transitions $^7F_{9/2} \rightarrow {}^6H_{15/2}$ involving the ground state $^6H_{15/2}$ are particularly relevant to correlate the crystal-field splitting with the anisotropic barrier. However, the greater number of transitions (12 or 13) with respect to the expected splitting into 8 components for the $^6H_{15/2}$ state, points out the presence of "hot bands" involving the first excited doublet of the $^7F_{9/2}$ levels,[20, 41] precluding an unambiguous determination of the crystal-field splitting. Note also that at room temperature, the solid-state emission spectrum for **2** exhibits the typical emission-lines for Dy^{3+} when excited at 370 nm (Fig. S12, Fig. S13), while, **1** presents a dual emission with both, a broad band of the ligands and the characteristic Dy^{3+} emission lines in the 565-585 nm region.

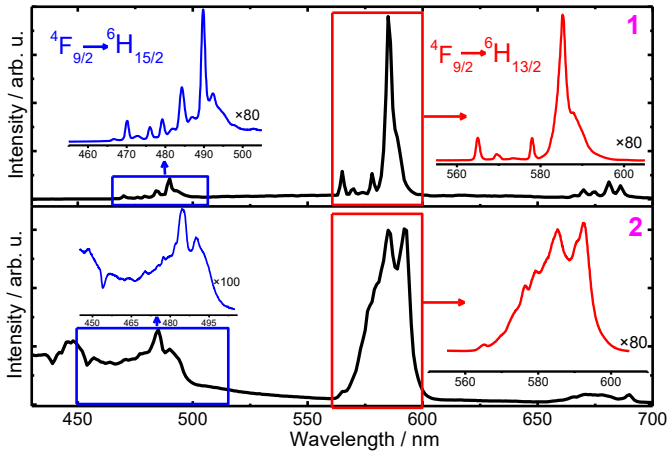

Fig. 4. Low temperature (77 K) solid-state emission spectra for **1** and **2** (λ_{exc} = 370 nm). The intra $4f^9$ Dy^{3+} transitions are reported.

In conclusion, two synthesised bifunctional cationic octahedral complexes $[DyR_2(py)_4][B(C_6H_5)_4]\cdot 2py$ and $[DyR_2(THF)_4][B(C_6H_5)_4]$ exhibiting a quasi linear (carbazolyl)N^--Dy-N^-(carbazolyl) angle in the axial direction exhibit a genuine SMM behaviour and a Dy^{3+}-based luminescence have been described. Important differences in the relaxation dynamics could be observed depending on the value of the angle in the axial direction as well as on the nature of the coordinated solvates in the equatorial plane. Appropriate substitution of such unexplored carbazolyl ligands may afford new synthetic routes to provide shorter Dy-ligand distances in the axial direction and in turn optimized SMMs with larger anisotropic barriers.

Conflicts of interest

There are no conflicts to declare.

Acknowledgements

The financial support of the Russian Science Foundation is highly acknowledged (Project № 17-73-30036). The French authors thank the University of Montpellier and CNRS for funding and PAC of ICGM for measurements.

Notes and references

1 J. Luzon and R. Sessoli, *Dalton Trans.*, 2012, **41**, 13556-13567.
2 D. N. Woodruff, R. E. P. Winpenny and R. A. Layfield, *Chem. Rev.*, 2013, **113**, 5110-5148.
3 F. Troiani and M. Affronte, *Chem. Soc. Rev.*, 2011, **40**, 3119-3129.
4 L. Bogani and W. Wernsdorfer, *Nat. Mater.*, 2008, **7**, 179-186.
5 N. F. Chilton, *Inorg. Chem.*, 2015, **54**, 2097-2099.
6 L. Ungur and L. F. Chibotaru, *Inorg. Chem.*, 2016, **55**, 10043-10056.
7 J. Liu, Y.-C. Chen, J.-L. Liu, V. Vieru, L. Ungur, J.-H. Jia, L. F. Chibotaru, Y. Lan, W. Wernsdorfer, S. Gao, X.-M. Chen and M.-L. Tong, *J. Am. Chem. Soc.*, 2016, **138**, 5441-5450.
8 S. K. Gupta, T. Rajeshkumar, G. Rajaraman and R. Murugavel, *Chem. Sci.*, 2016, **7**, 5181-5191.
9 M. Gregson, N. F. Chilton, A.-M. Ariciu, F. Tuna, I. F. Crowe, W. Lewis, A. J. Blake, D. Collison, E. J. L. McInnes, R. E. P. Winpenny and S. T. Liddle, *Chem. Sci.*, 2016, **7**, 155-165.
10 Y.-C. Chen, J.-L. Liu, L. Ungur, J. Liu, Q.-W. Li, L.-F. Wang, Z.-P. Ni, L. F. Chibotaru, X.-M. Chen and M.-L. Tong, *J. Am. Chem. Soc.*, 2016, **138**, 2829-2837.
11 Y.-S. Ding, N. F. Chilton, R. E. P. Winpenny and Y.-Z. Zheng, *Angew. Chem. Int. Edit.*, 2016, **55**, 16071-16074.
12 Y.-S. Meng, L. Xu, J. Xiong, Q. Yuan, T. Liu, B.-W. Wang and S. Gao, *Angew. Chem. Int. Edit.*, 2018, **57**, 4673-4676.
13 F. S. Guo, B. M. Day, Y. C. Chen, M. L. Tong, A. Mansikkamaki and R. A. Layfield, *Angew. Chem. Int. Ed. Engl.*, 2017, **56**, 11445-11449.
14 C. A. P. Goodwin, F. Ortu, D. Reta, N. F. Chilton and D. P. Mills, *Nature*, 2017, **548**, 439-442.
15 F.-S. Guo, B. M. Day, Y.-C. Chen, M.-L. Tong, A. Mansikkamäki and R. A. Layfield, *Science*, 2018, **362**, 1400-1403.
16 J. Tang and P. Zhang, in *Lanthanide Single Molecule Magnets*, Springer Berlin Heidelberg, Berlin, Heidelberg, 2015, DOI: 10.1007/978-3-662-46999-6_2, pp. 41-90.
17 R. A. Layfield and M. Murugesu, *Lanthanides and Actinides in Molecular Magnetism*, Wiley, 2015.
18 A. Lunghi, F. Totti, R. Sessoli and S. Sanvito, *Nat. Comm.*, 2017, **8**, 14620.
19 L. Escalera-Moreno, J. J. Baldoví, A. Gaita-Ariño and E. Coronado, *Chem. Sci.*, 2018, **9**, 3265-3275.
20 J. Long, Y. Guari, R. A. S. Ferreira, L. D. Carlos and J. Larionova, *Coord. Chem. Rev.*, 2018, **363**, 57-70.
21 J.-H. Jia, Q.-W. Li, Y.-C. Chen, J.-L. Liu and M.-L. Tong, *Coord. Chem. Rev.*, 2019, **378**, 365-381.
22 B.-C. Liu, N. Ge, Y.-Q. Zhai, T. Zhang, Y.-S. Ding and Y.-Z. Zheng, *Chem. Commun.*, 2019, **55**, 9355-9358.
23 D. L. Kays, *Chem. Soc. Rev.*, 2016, **45**, 1004-1018.
24 F. K.-W. Kong, M.-C. Tang, Y.-C. Wong, M.-Y. Chan and V. W.-W. Yam, *J. Am. Chem. Soc.*, 2016, **138**, 6281-6291.
25 S. Shi, M. C. Jung, C. Coburn, A. Tadle, D. Sylvinson M. R, P. I. Djurovich, S. R. Forrest and M. E. Thompson, *J. Am. Chem. Soc.*, 2019, **141**, 3576-3588.
26 R. Hamze, S. Shi, S. C. Kapper, D. S. Muthiah Ravinson, L. Estergreen, M.-C. Jung, A. C. Tadle, R. Haiges, P. I. Djurovich, J. L. Peltier, R. Jazzar, G. Bertrand, S. E. Bradforth and M. E. Thompson, *J. Am. Chem. Soc.*, 2019, **141**, 8616-8626.
27 L. Gajecki, D. J. Berg, J. Hoenisch and A. G. Oliver, *Dalton Trans.*, 2018, **47**, 15487-15496.
28 K. Müller-Buschbaum and Catharina C. Quitmann, *Eur. J. Inorg. Chem.*, 2004, **2004**, 4330-4337.
29 W. J. Evans, G. W. Rabe and J. W. Ziller, *Organometallics*, 1994, **13**, 1641-1645.
30 K. Müller-Buschbaum and A. Zurawski, *Z. Anorg. Allg. Chem.*, 2007, **633**, 2300-2304.

31 K. R. Meihaus, S. G. Minasian, W. W. Lukens, S. A. Kozimor, D. K. Shuh, T. Tyliszczak and J. R. Long, *J. Am. Chem. Soc.*, 2014, **136**, 6056-6068.
32 P. L. Scott and C. D. Jeffries, *Phys. Rev.*, 1962, **127**, 32-51.
33 N. F. Chilton, D. Collison, E. J. L. McInnes, R. E. P. Winpenny and A. Soncini, *Nat. Commun.*, 2013, **4**, 2551.
34 J. Long, I. V. Basalov, N. V. Forosenko, K. A. Lyssenko, E. Mamontova, A. V. Cherkasov, M. Damjanović, L. F. Chibotaru, Y. Guari, J. Larionova and A. A. Trifonov, *Chem. Eur. J.*, 2019, **25**, 474-478.
35 K. R. Meihaus, J. D. Rinehart and J. R. Long, *Inorg. Chem.*, 2011, **50**, 8484-8489.
36 S.-S. Liu, Y.-S. Meng, Y.-Q. Zhang, Z.-S. Meng, K. Lang, Z.-L. Zhu, C.-F. Shang, B.-W. Wang and S. Gao, *Inorg. Chem.*, 2017, **56**, 7320-7323.
37 J.-L. Liu, K. Yuan, J.-D. Leng, L. Ungur, W. Wernsdorfer, F.-S. Guo, L. F. Chibotaru and M.-L. Tong, *Inorg. Chem.*, 2012, **51**, 8538-8544.
38 S. N. König, N. F. Chilton, C. Maichle-Mössmer, E. M. Pineda, T. Pugh, R. Anwander and R. A. Layfield, *Dalton Trans.*, 2014, **43**, 3035-3038.
39 M. Guo and J. Tang, *Inorganics*, 2018, **6**, 16.
40 J. Long, D. Lyubov, T. Mahrova, A. Cherkasov, G. K. Fukin, Y. Guari, J. Larionova and A. Trifonov, *Dalton Trans.*, 2018, **47**, 5153-5156.
41 J. Long, *Frontiers in Chemistry*, 2019, **7**, 63.